Published in final edited form as:
Biochemistry. 2009 September 22; 48(37): 8899–8907. doi:10.1021/bi900979b.

Cloning and Epitope Mapping of Cry11Aa-Binding Sites in the Cry11Aa-Receptor Alkaline Phosphatase from *Aedes aegypti*†

Luisa E. Fernandez[§,‡], **Claudia Martinez-Anaya**[§,‡], **Erandi Lira**[§], **Jianwu Chen**[||], **Amy Evans**[||], **Salvador Hernández-Martínez**[⊥], **Humberto Lanz-Mendoza**[⊥], **Alejandra Bravo**[§], **Sarjeet S. Gill**[||], and **Mario Soberón**[§,*]

[§]Instituto de Biotecnología, Universidad Nacional Autónoma de México, Apdo, postal 510-3, Cuernavaca 62250, Morelos, Mexico

[||]Department of Cell Biology and Neuroscience, University of California, Riverside, California 92521

[⊥]Centro de Investigaciones sobre Enfermedades Infecciosas, Instituto Nacional de Salud Pública, Cuernavaca, Morelos, Mexico

Abstract

Cry11Aa is the most active *Bacillus thuringiensis israelensis* toxin against *Aedes aegypti* larvae. *Ae. aegypti* alkaline phosphatase (ALP) was previously identified as a Cry11Aa receptor mediating toxicity. Here we report the cloning and functional characterization of this *Ae. aegypti* Cry11Aa-ALP receptor. Of three ALP's cDNA clones, the recombinant produced ALP1 isoform was shown to bind Cry11Aa and P1.BBMV peptide phage that specifically binds the midgut ALP-Cry11Aa receptor. An anti-ALP1 antibody inhibited binding to brush border membrane vesicles and toxicity of Cry11Aa in isolated cultured guts. Two ALP1 Cry11Aa binding regions (R59–G102 and N257–I296) were mapped by characterizing binding of Cry11Aa to nine recombinant overlapping peptides covering the ALP1 sequence. Finally, by using a peptide spot array of Cry11Aa domain III and site-directed mutagenesis, we show that the ALP1 R59–G102 region binds Cry11Aa through domain II loop α-8 while ALP1 N257–I296 interacts with Cry11Aa through domain III ^{561}RVQSQNSGNN^{570} located in β18-β19. Our results show that Cry11Aa domain II and domain III are involved in the binding with two distinct binding sites in the ALP1 receptor.

Bacillus thuringiesis (Bt)[1]Cry toxins are used worldwide for the control of insect pests in agriculture and in public health. The family of Cry toxins includes more than 200 toxins with different specificities against various insect orders and nematodes (1). Despite the large number of Cry toxins characterized so far, only a few are used in commercial insecticidal products (2).

One of the most successful applications of Bt is the control of mosquito vectors of dengue and malaria, human diseases that cause the death of millions annually. The Bt strain subsp.

†Research was funded in part through grants from the National Institutes of Health, 1R01 AI066014, DGAPA/UNAM IN218608 and IN210208-N, CONACyT U48631-Q.

*Corresponding author. mario@ibt.unam.mx. Phone: 52 777 3291618. Fax: 52 777 3172388.
‡Both authors contributed equally to this work.

[1]Abbreviations: ALP, alkaline phosphates; APN, aminopeptidase-N; BBMV, brush border membrane vesicles; Bt, *Bacillus thuringiensis*; Bti, *Bacillus thuringiensis israelensis*; Cry, crystal proteins; PMSF, phenylmethanesulfonyl fluoride; ELISA, enzyme-linked immunosorbent assay; TRX, thioredoxin protein; NHE3, midgut sodium–proton exchanger.

israelensis (Bti) is highly active against several mosquito species including *Aedes aegypti*, a transmission vector of dengue fever, yellow fever, and chikungunya fever viruses (3). Bti produces at least six different toxins that belong to two distinct Bt toxin families: the three-domain Cry family (Cry4Aa, Cry4Ba, Cry10Aa, and Cry11Aa) and the Cyt family (Cyt1Aa and Cyt2Ba).

The structures of several three-domain Cry toxins with different insect specificities have been solved and shown to be composed of three distinct domains (1). These protein structures show important similarities despite the fact that they share low amino acid sequence identity. The amino-terminal domain I is composed of seven α-helices and is involved in membrane insertion and oligomerization, domain II, formed by three β-sheets that are connected by exposed loops in the apex, has been shown to be involved in receptor binding, while domain III, a β-sandwich, is also involved in receptor interaction (1).

The mechanism of action of Cry1A toxins that are active against lepidopteran insects has been described in detail and shown to involve sequential interaction with at least two insect proteins located in microvilli of larval gut (1, 4). Cry1A are produced as 130 kDa protoxins that are proteolytically activated by midgut proteases to yield 60 kDa toxins. The activated Cry1A toxins bind first to cadherin receptor by exposed domain II loops α-8, -2, and -3 (5–7). Cadherin binding facilitates additional proteolysis by an uncharacterized protease at the amino terminus, resulting in cleavage of α-helix 1 and formation of a 250 kDa oligomer (8). Finally, the oligomer binds to GPI-anchored proteins, such as aminopeptidase-N (APN) or alkaline phosphatase (ALP), through a domain III binding epitope in β-16 and also by exposed loops of domain II (6). These GPI-anchored receptors are located in lipid rafts where the oligomeric toxin inserts and forms pores that cause cell lysis and insect death (4, 9).

In the case of mosquitocidal Cry toxins, it is proposed that the mechanism of action is conserved since similar molecules in larvae midgut have been identified as Cry toxin binding molecules, like a cadherin of *Anopheles gambiae* that binds Cry4-Ba (10), or GPI-anchored proteins such as APN in *Anopheles quadrimaculatus* and *A. gambiae* that bind Cry11Ba (11, 12), or an ALP in *Ae. aegypti* that binds Cry11Aa toxin (13). Furthermore, domain II loop regions of Cry4Aa, Cry4Ba, and Cry11Aa have been shown to be important for binding to midgut membranes and toxicity, and in Cry11Aa loop α-8 of domain II is involved in the interaction with *Ae. aegypti* ALP (13–16). In addition, Cry11Aa forms a 250 kDa oligomer after activation with trypsin in the presence of brush border membrane vesicles (BBMV), and this prepore oligomer is efficient in pore-formation activity in contrast with the monomeric Cry11Aa toxin (17).

In order to understand the molecular basis of insect specificity and the mode of action of mosquitocidal Cry11Aa toxin, we decided to further characterize the Cry11Aa–*Ae. aegypti* ALP interaction. Here we report the cloning and functional characterization of the *Ae. aegyti* ALP–Cry11Aa receptor. We also mapped the binding sites both in Cry11Aa and in the receptor revealing that Cry11Aa domains II and III are each involved in binding two distinct ALP regions.

EXPERIMENTAL PROCEDURES

Site-Directed Mutagenesis of the cry11Aa Gene

Mutagenesis of the pGC6 plasmid that encodes the *cry11Aa* gene (18) was performed using the QuikChange XL kit (Stratagene, La Jolla, CA). Appropriate oligonucleotides were synthesized for each mutant construction. Mutants were sequenced and transformed into acrystalliferous Bt strain 407 (19).

Toxin Cry11Aa Purification and Activation

Bt strains harboring pCG6 or *cry11Aa* mutants were grown for 72 h in sporulation medium (20) plus erythromycin (25 μg/mL) at 200 rpm and 30 °C until complete sporulation. The spores and crystals were harvested and washed three times with buffer containing 1 mM EDTA, 0.1 mM phenylmethanesulfonyl fluoride (PMSF), 1 μg/mL pepstatin, and 5 μg/mL leupectin in PBS (150 mM NaCl, 2.8 mM NaH_2PO_4, 4mM$Na_2HPO_4 \cdot 7H_2O$, pH 7.2). Crystals were isolated by sucrose gradients as previously described (21). The crystals were recovered in 50 mM Tris, pH 8, and 1 mM PMSF, solubilized for 1 h at 4 °C with 0.1M NaOH, and then activated with trypsin (1:50 w/w) for 2 h at 25 °C.

Toxicity ex Vivo Assays with Cultured Guts

Mosquito guts were cultured as previously described with some modifications (22). Briefly, third instar larval guts were dissected in a drop of PBS containing 1 mM PMSF, 1 mM EDTA, and 0.1 mM leupeptin and washed thoroughly with this buffer. Two midguts per well were placed in a 96-well culture plate (Nalgene Nunc Co., Naperville, IL) containing 100 μL of Schneider's *Drosophila* medium (Gibco, Invitrogen). Cry11Aa protoxin (1 μg) with or without anti-ALP1 (1:1000) or anti-NHE3 (1:1000) antibodies was added to the cultured guts and left at room temperature for 18 h. When antibodies were included in the assays, the cultured guts were incubated for 30 min with the antibody before addition of Cry11Aa protoxin. Then lactate dehydrogenase (LDH) release was determined using Cytotox 96, a nonradioactive cytotoxicity assay (Promega, Madison, WI) as follows. Fifty microliters of medium was transferred to a 96-well ELISA plate to which 50 μL of assay solution was added per medium sample and incubated for 30 min at room temperature. Fifty microliters of stop solution was added per well and absorbance at 490 nm recorded with a microplate reader from Molecular Devices (Sunnyvale, CA). For positive controls of LDH release, 3 μL of 10× lysis solution was added to the cultured guts and incubated for 15 min at room temperature. Three replicates per treatment were recorded.

Cloning of ALP cDNAs and Their Expression

Full-length ALP1 and ALP3 cDNAs were isolated from an *Ae. aegypti* cDNA library constructed in pSPORT1 (Invitrogen) as previously described (23). To obtain ALP2, 5′ and 3′ RACE were performed using *Aedes* midgut cDNA and primers based on the *Ae. aegypti* genome (http://aaegypti.vectorbase.org). In addition, an internal fragment that overlapped the two RACE products was similarly obtained, and the three fragments were then used to construct a full-length ALP2 cDNA.

For protein expression the three cDNAs were either cut using available restriction enzyme sites (ALP1 and ALP2) or amplified using specific primers (ALP3) to obtain fragments that when expressed would not have the N-terminal peptide signal sequence. These fragments were then cloned into expression vector, pQE30 (Qiagen, Valencia, CA). The fragments were fully sequenced at the Institute of Integrative Genome Biology, University of California, Riverside. The final constructs in pQE30 were transformed into the *Escherichia coli* strain M15 (pREP4). ALP1 was also cloned into plasmid pET-32b to produce it as a fusion protein with thioredoxin using appropriate primer sequences and transformed into *E. coli* strain ER2566. Protein expression was induced by addition of 1mM isopropyl β-D-thiogalactoside (IPTG). The N-terminal 6× His-tagged recombinant proteins were solubilized and purified in urea using Ni-NTA resin (Qiagen, Valencia, CA) and resolved in SDS–PAGE.

For antibody production, the purified 6× His-tagged ALP1 protein produced using pQE30 was separated by SDS–PAGE, and the gels were stained and then destained. Purified protein

bands were excised from the gel, washed three times with water, and then used to immunize rabbits for antibody development according to standard protocols.

Construction and Expression of Overlapping ALP1 Peptides

Nine overlapping peptide fragments of 150 residues (P1–P9) that cover the whole ALP1 amino acid sequence were amplified by PCR using the primer sequences described in Table 1 and theALP1 clone as template. The PCR products were purified with the QIAquick PCR purification kit (Qiagen, Valencia, CA), digested with *Bgl*II and *Hin*dIII restriction enzymes, and ligated into pET-32b expression vector previously digested with the same restriction enzymes. Ligation mixtures were transformed into strain ER2566. After cloning complete nucleotide sequences of the nine fragments were obtained revealing no mutations.

E. coli ER2566 cultures were grown at 37 °C in 2× TY (supplemented with 100 μg/mL ampicillin and 0.1% glucose) to an OD of 0.7 at 600 nm, and protein expression of ALP1 fragments was induced by adding 0.5 mM IPTG followed by a further incubation for 4 h at 25 °C. All ALP1 fragments were solubilized from inclusion bodies with 8 M urea and 300 mM Tris-HCl, pH 8. The solubilized fragments were applied to a Ni-agarose column (Qiagen, Germany) and washed with PBS, and the ALP1 fragments were eluted with 2 mL of 250m Mimidazole and 0.2% azide in PBS.

Preparation of Brush Border Membrane Vesicles (BBMV)

BBMV were prepared from dissected midguts of fourth instar *Ae. aegypti* larvae by differential precipitation using $MgCl_2$ as previously reported (24) and stored at −70 °C until used.

Qualitative Assays of Cry11Aa Binding to BBMV

Cry11Aa toxin was biotinylated using biotinyl-*N*-hydroxysuccinimide ester (Amersham Pharmacia Biotech). Binding was performed in 100 μL of binding buffer (1× PBS, 01% BSA, 0.1%Tween 20, pH 7.6). After incubation of 10 nM labeled toxin with 10 μg of *Ae. aegypti* BBMV for 1 h at 25 °C, unbound toxin was removed by centrifugation (10 min at 14000*g*). The membrane pellet with bound toxin was washed twice with 100 μL of binding buffer and suspended in 1× PBS, pH 7.6. An equal volume of 2× sample loading buffer (0.125 M Tris-HCl, pH 6.8, 4% SDS, 20% glycerol, 10%2-mercaptoethanol, 0.01% bromophenol blue) was added; samples were boiled for 3 min, separated by SDS–PAGE (10%), and electrotransferred to nitrocellulose membranes. The biotinylated protein was visualized by incubation with streptavidin–peroxidase conjugate (1:6000 dilution) for 1 h, followed by incubation with luminol (Pierce, Rockford, IL) as described by the manufacturer. For competition assays biotinylated Cry11Aa was preincubated with peptides or antibodies for 1 h at room temperature before incubation with BBMV.

Toxin Overlay Assay

Peptides (1 μg) were separated in 15% SDS–PAGE and electrotransferred to Hybond-ECL membranes. After blocking, the membranes were incubated for 2 h with 10 nM biotinylated Cry11Aa or mutant proteins, and the bound protein was revealed with streptavidin–peroxidase as described above.

Enzyme-Linked Immunosorbent Assay (ELISA)

ELISA 96-well plates (Costar, NY) were incubated for 12 h at 4 °C with 0.5 μg/mL corresponding ALP recombinant protein (ALP1, ALP2, ALP3) in 50 mM $NaHCO_3$ pH 9.6, followed by five washes with PBS and 0.2% Tween 20. The plates were then incubated with PBS, 0.5%gelatin (Bio-Rad) and 0.2%Tween 20 for 1 h at 37 °C and washed five times with

buffer A (PBS, 0.1% Tween 20). The ELISA plates were incubated with biotinylated Cry11Aa or Cry11Aa mutants (5 nM), biotinylated Cry4Ba (5 nM), or P1.BBMV (10^{10} PFU) for 2 h at 37 °C and washed again with buffer A. Cry proteins that boundALP1 were detected with streptavidin–peroxidase conjugate (Amersham Bioscience) for 1 h. In the case of P1.BBMV, plates were incubated with anti-M13 antibody (1:2000) in blocking solution for 1 h at room temperature. The plates were then washed three times with washing buffer and incubated with anti-mouse HRP antibody (1:2000), and finally, plates were incubated with 2 mM *o*-phenylenediamine and 0.7% H_2O_2 in 0.1 M Na_2HPO_4, pH5. The enzymatic reaction was stopped with 6 N HCl and absorbance read at 490 nm with a microplate reader from Molecular Devices (Sunnyvale, CA).

ALP1 Binding to Cellulose Membrane-Bound Peptides

Fifty-seven cellulose-bound peptides of Cry11Aa domain III (I462–K643) were prepared by Jerini AG(Peptide Technologies, Berlin) by automated spot synthesis (25). Membrane-bound peptides were washed with ethanol and then with Tris-buffered saline (TBS; 50 mM Tris, 137 mM NaCl, 2.7 mM KCl, pH 8) before blocking for 16 h at 4 °C with TBS, 0.1% Tween 20, and 5% skim milk. The membrane was washed with TBS and 0.1% Tween 20 and incubated afterward with 20 μg/mL ALP1 in TBS and 0.1%Tween 20 at 4 °C for 4 h and detected with anti-ALP1 antibody (1:2000). After three washes with TBS and 0.1%Tween 20 the membrane was incubated with anti-mouse HRP antibody (1:2000) followed by incubation with luminol and visualized with SuperSignal chemiluminescence substrate (Pierce, Rockford, IL).

Insect Bioassays

Ten early fourth instar *Ae. aegypti* larvae reared at 28 °C, 87%humidity, and 12:12 light:dark were placed in 100 mL of dechlorinated water. The effect of Cry11Aa toxin and different mutants on mortality was analyzed after 24 h. The mean lethal concentration (LC_{50}) was estimated by Probit analysis using statistical parameters after four independent assays (Polo-PC LeOra Software).

RESULTS

Cloning of Ae. aegypti ALP That Binds Cry11Aa

Previously, we reported the construction of an EST library from RNA samples of *Ae. aegypti* larvae Malpighian tubules and midgut tissue (23). Analysis of DNA sequences of random clones from this library by BlastX revealed at least two different ALP transcripts (ALP1 and ALP3). In addition, Blast analysis of the *Ae. aegypti* genome database revealed a third ALP gene (ALP2) that was also expressed in the midgut library and cloned using appropriate oligonucleotides (Experimental Procedures). Full-length cDNAs of the three ALP clones excluding signal peptides sequences were cloned into pQE30 and produced in *E. coli*. We also previously reported a peptide phage (P1.BBMV) selected by biopanning against *Ae. aegypti* BBMV that specifically recognized the 65 kDa ALP protein that is a receptor of Cry11Aa. This phage competed Cry11Aa binding to midgut tissue sections and inhibited Cry11Aa toxicity (13). Therefore, we took advantage of this specific peptide phage to identify the cDNA clone coding for the midgut ALP protein. ELISA binding assays showed that ALP1 bound Cry11Aa, Cry4Ba, and P1.BBMV phage. In contrast, ALP2 and ALP3 proteins showed poor or no binding to the Cry toxins and the P1.BBMV phage (Figure 1).

Analysis of the translated DNA sequence of ALP1 revealed an open reading frame of 542 residues with a predicted molecular mass of 59.5 kDa, p*I* of 6.8, and nine potential glycosylation sites. Glycosylation may account for the differences of the predicted and the

observed molecular mass in the native 65 kDa ALP (13). The ALP1 sequence corresponds to the *Ae. aegypti* ALP gene bank accession number (gb.) EAT39089. However, ALP EAT39089 codes for an open reading frame of only 513 residues. The ALP1 amino acid region V30–K58 is not present in the EAT39089 sequence most probably due to incorrect annotation since the rest of the protein sequence is identical.

ALP1 shows amino acid sequence similarities with ALPs from *Culex quinquefasciatus* (75% identity, gb. EDS32226), *A. gambiae* (66% identity, gb. EAA03918), *Tribolium castaneum* (48% identity, gb. XP_971418.1), and *Heliothis virescens* (47% identity, gb. ACP39712) (26). Figure 2 shows an alignment of the *Ae. aegypti* ALP1 amino acid sequence with ALPs from the insects mentioned above. ALP's are homodimeric metalloenzymes that catalyze the hydrolysis or the phosphotransfer of monophosphoesters. Each monomer contains a catalytic site with conserved catalytic serine and arginine residues and conserved residues for three metal binding sites, M1, M2, and M3 that bind two zinc atoms and one magnesium atom, respectively (27). The metal binding sites are comprised of two histidines and one aspartate residue for M1, one histidine and two aspartates for M2, and one aspartate, one glutamate, and a threonine that in some ALP's is substituted by a serine for M3. ALP1 has a 23 amino acid N-terminal signal peptide and also a predicted GPI anchor site (S515). In addition, ALP1 contains catalytic serine (S153) and arginine (R229) residues and residues involved in metal binding in M1 (H383, D379, and H497), M2 (D103, D420, and H421), and M3 (D103, S217, and E374) (Figure 2).

ALP1 Is Involved in Cry11Aa Toxicity

To determine the role of ALP1 in Cry11Aa binding and toxicity, we raised a polyclonal antibody against the recombinant ALP1 to use it in competition binding assays and to inhibit Cry11Aa toxicity, and we also analyzed the effect of a control antibody that was raised against the larval midgut sodium–proton exchanger NHE3 of this mosquito species. To determine the specificity of the antibodies used in competition experiments, we analyzed the binding of these antibodies to BBMV proteins by Western blot. Figure 3A shows that the anti-ALP1 antibody only recognized a 65 kDa band that was previously shown to correspond to the ALPCry11Aa receptor while the anti-NHE3 antibody recognized two bands of 150 and 120 kDa. NHE3 encodes for a 130 kDa protein which is both glycosylated and phosphorylated, and the two bands probably represent modified and unmodified forms of the proton exchanger (S. S. Gill, unpublished results). Binding of trypsin-activated biotinylated Cry11Aa to *Ae. aegypti* BBMV was performed in the presence of the anti-ALP1 antibody. When treated with trypsin, Cry11Aa protoxin is cleaved into two fragments of 36 and 32 kDa that remain associated and retain toxicity (28). Figure 3B showsCry11Aa binding was competed by the anti-ALP1 antibody while the anti-NHE3 antibody only displaced 30% of the Cry11Aa binding as judged by scanning the optical density of the Cry11Aa 36 kDa protein band.

To assess the toxicity of Cry11Aa on midgut tissue, we used an *ex vivo* toxicity assay using cultured larval guts that were exposed to Cry11Aa protoxins. This assay relies on the quantification of LDH release by larval guts after toxin exposure (Experimental Procedures). Figure 3C shows the anti-ALP1 antibody inhibited 90% of LDH release while the control anti-NHE3 antibody protected 50% of LDH release after toxin treatment.

Two Binding Sites of ALP1 Play a Role in Its Interaction with Cry11Aa

In order to map the Cry11Aa binding sites in ALP1, we constructed nine overlapping ALP1 peptides of 150 residues each, in such a way that each peptide had a 100-residue overlap with the previous peptide. ALP1 and the DNA fragment of each peptide were cloned into pET-32b and expressed in *E. coli* as a fusion protein with thioredoxin protein (TRX).

Biotinylated Cry11Aa bound ALP1–TRX but not thioredoxin in ligand blot assay (data not shown). Binding of biotinylated Cry11Aa to the purified peptides was performed by ligand blot assays. Figure 4A shows Cry11Aa bound peptides P1, P2, P4, P5, and P6. Peptides P1 and P2 share the amino acid region R59–G102 while P4, P5, and P6 share the amino acid region N257–I296 (underlined in Figure 2), indicating these two ALP regions are involved in Cry11Aa binding.

To determine if both ALP1 binding sites are involved in Cry11Aa binding to BBMV, we analyzed toxin binding to BBMV in the presence of peptides P2 and P5 using peptide P8 as a control. Figure 4B shows that both P2 and P5 peptides competed with Cry11Aa binding to BBMV while P8 did not. A mixture of P2 and P5 improved binding competition although recombinant ALP1–TRX was more efficient in competing with Cry11Aa binding to BBMV (Figure 4B).

Domains II and III of Cry11Aa Are Involved in ALP Binding

ALP1 contains at least two Cry11Aa binding sites, one of which could interact with loop α-8 from domain II, since a synthetic peptide with sequence corresponding to loop α-8 of Cry11Aa competed with the binding of P1.BBMV to midgut tissue sections (13). In a previous work (15) we selected two peptide phages (P1.tox and P5.tox) that bound to Cry11Aa toxin and competed binding of Cry11Aa to BBMV and inhibit toxicity to *Ae. aegypti* larvae. The peptide phage P5.tox binds domain II loop α-8. We then isolated point mutants in loop α-8 demonstrating that this region is involved in binding to BBMV and in toxicity against *Ae. aegypti* (15). However, the binding site of peptide phage P1.tox remained elusive. Ligand blot assays indicated P1.tox phage binds the 32 kDa fragment and not the 36 kDa fragment of trypsin-activated Cry11Aa toxin (data not shown). Since the 32 kDa fragment contains the C-terminal end of the toxin including all of domain III (28), we propose that P1. tox phage may recognize a region located in domain III. To determine if Cry11Aa domain III sequences are involved in binding with ALP1, a library of overlapping peptides derived from domain III (I462–K643) was created using a peptide-spot synthesis technique (25). Fifty-seven peptides of 15 amino acids each (12 residues overlap with the previous peptide) were bound to the nitrocellulose membrane and screened with labeled ALP1 as described in Experimental Procedures. Binding of ALP1 to the peptide array revealed an amino acid region comprised of residues ^{561}RVQSQNSGNN^{570} (spots 33, 34, and 35) (Figure 5). Based on a model of the structure of Cry11Aa that was previously constructed (15), amino acids ^{561}RVQSQNSGNN ^{570} are located in β18-β19 and are exposed to the solvent (15). These data suggest that domain III residues ^{561}RVQSQNSGNN^{570} might be involved in the binding interaction of Cry11Aa toxin to ALP1.

To further study the role of the domain III ^{561}RVQSQNSGNN ^{570} region on binding with ALP1 and in toxicity, we performed site-directed mutagenesis of this region and created two Cry11Aa mutants, QSQ563–565AAA and NSG566–568AAA. The two mutants produced crystals as wild-type Cry11Aa and upon activation with trypsin produced the expected 36 and 32 kDa bands, indicating these mutations did not affect protein structure that render proteins more susceptible to proteolysis (data not shown). The two mutants showed a 3-fold reduction in toxicity against *Ae. aegypti* larvae (Table 2). We determined the binding of the two Cry11Aa mutants, QSQ563–565AAA and NSG566–568AAA, to ALP1 by ELISA. We also included mutant E266A located in domain II loop α-8, which as mentioned above has lower larval toxicity and binding to *Ae. aegypti* BBMV (15). All three mutants showed reduced binding to ALP1–TRX in comparison with wild-type Cry11Aa (Figure 6A).

Finally, in order to identify binding epitopes in ALP1 that are recognized by loop α-8 and by the domain III ^{561}RVQSQNSGNR^{570} region of Cry11A, we performed ligand blot

assays of mutant E266A (located in loop α-8) and mutant QSQ563–565AAA (located in domain III) to the nine ALP1-overlapping peptides described above. Mutant E266A has reduced binding to the P1 and P2 peptides (Figure 6B) while mutant QSQ563–565AAA shows reduced binding to the P4, P5, and P6 peptides (Figure 6C). These results demonstrated that loop α-8 binds ALP1 through the R59–G102 region while domain III ^{561}RVQSQNSGNN^{570} binds ALP1 through the N257–I296 region.

DISCUSSION

As mentioned above, the three-domain Cry toxins are a large family of proteins toxic to different insect orders. Even though different members of this family of proteins share low sequence identity, they share a similar three-domain structure suggesting these toxins may share a conserved mode of action. It is then proposed that in different insect orders a similar sequence of events will render Cry proteins from soluble activated toxins to membrane inserted pores that cause osmotic lysis of midgut cells and insect death. However, what is somehow surprising is that similar insect midgut proteins seem to participate in binding and toxicity of Cry toxins in different insect orders. These data may reflect that similar midgut protein components are present in different insect orders and thus were selected as toxin receptors. Alternatively, the interaction of Cry toxins with these protein targets may indicate that binding to proteins with particular function (APN, ALP, cadherin) in the physiology of the insect gut is critical for Cry toxicity. For instance, binding of Cry1Ac or Cry11Aa toxins to their corresponding ALP receptors in lepidopteran or dipterans insects lowered ALP enzymatic activity (13, 29). However, proteins like a 270 kDa glycoprotein in *Lymantria dispar* (30), a GPI-anchored ADAM metalloprotease in *Lepinotarsa decemlineata* (31), or a GPI-anchored glucosidase in *A. albimanus* (Fernandez-Luna and Miranda, unpublished) can also function as toxin receptors. Thus a wide variety of proteins with differing function may participate in Cry toxin action.

Here we report the cloning and functional characterization of the *Ae. aegypti* Cry11Aa-ALP receptor. We identified three ALP cDNA clones, one of which (ALP1) bound Cry11Aa, Cry4Ba, and the peptide phage P1.BBMV. We show that ALP1 is a functional Cry11Aa receptor involved in toxicity since recombinant ALP1–TRX competed with Cry11Aa binding to BBMV. Furthermore, a polyclonal anti-ALP1 antibody competed binding of Cry11Aa to *Ae. aegypti* BBMV and inhibited Cry11Aa toxicity in *ex vivo* toxicity assays with cultured guts. As control antibody we analyzed the effect of an antibody that recognizes a larval midgut sodium–proton exchanger (NHE3). The anti-NHE3 antibody competed Cry11Aa binding to some extent (30%) as judged by scanning the Cry11Aa 36 kDa band (Figure 3B) and showed some protection of Cry11Aa toxicity (50% protection) although not as high as that shown by anti-ALP1 (90%protection). We have no definite explanation for the marginal protective effect shown by anti-NHE3 antibody, although this may be a background effect due to nonspecific interactions between antiserum and gut proteins.

Regarding the binding events that occur during interaction of Cry toxins with receptors, it has been shown that binding of Cry1A toxins to cadherin receptor in lepidopteran insects is a complex event that involves three exposed loops of domain II. The binding epitopes of mosquitocidal toxins with cadherin receptor have not been mapped yet, although in the case of *Ae. aegypti* cadherin it involves at least Cry11Aa domain II loop α-8 (Chen and Gill, submitted). In the case of lepidopteran GPI-anchored APN, not only are Cry1Ab or Cry1Ac domain II loop regions involved in APN binding interaction but domain III exposed regions are also important in the interaction of Cry1A toxins with APN (6, 31). A sequential binding mechanism for Cry1Ac interaction with *L. dispar* APN was proposed where Cry1Ac domain III participates in initial binding to APN that favors the subsequent binding of domain II exposed loops with a different site of APN (32). Here we show that in *Ae. aegypti* the ALP1

receptor contains at least two different toxin-binding sites comprised by residues R59–G102 and N257–I296 that bind Cry11Aa through domain II loop α-8 and domain III ^{561}RVQSQNSGNN ^{570} amino acid regions, respectively. However, we cannot exclude that additional binding regions are involved in the binding ofCry11Aa toALP1 especially sinceCry11Aa binding to BBMV was not completely competed by ALP1 peptides P2 and P5 as did ALP1 (Figure 4B). In addition, we cannot exclude sugar-mediated interactions between Cry toxin and ALP1 that would have not been revealed since a recombinant *E. coli* produced ALP1 was used in our binding assays.

These results indicate that domain III and domain II exposed regions are involved in the binding interaction with the GPI-anchored ALP receptor. The proposed role for GPI-anchored receptors in the mode of action of Cry toxins is to facilitate toxin oligomer membrane insertion in lipid rafts (33). The fact that similar structural regions in nonrelated Cry toxins (Cry1Ac vs Cry11Aa) are involved in the binding with different GPI-anchored receptors (APN vs ALP) in two different insect orders suggests that the mechanism of action of Cry toxins is highly conserved at least in dipteran and lepidopteran insect orders and that Cry1A and Cry11A pass through a similar sequence of events from soluble activated toxins to membrane-inserted pores.

Acknowledgments

We thank Lizbeth Cabrera and Jorge Sanchez for technical assistance.

References

1. Bravo A, Gill SS, Soberón M. Mode of action of *Bacillus thuringiensis* toxins and their potential for insect control. Toxicon. 2007; 49:423–435. [PubMed: 17198720]
2. Soberón M, Gill SS, Bravo A. Signaling versus punching hole: How do *Bacillus thuringiensis* toxins kill insect midgut cells? Cell Mol Life Sci. 2009; 66:1337–1349. [PubMed: 19132293]
3. Chhabra M, Mittal V, Bhattacharya D, Rana U, Lal S. Chikungunya fever: A re-emerging viral infection. Indian J Med Microbiol. 2008; 26:5–12. [PubMed: 18227590]
4. Bravo A, Gómez I, Conde J, Muñoz-Garay C, Sánchez J, Miranda R, Zhuang M, Gill SS, Soberón M. Oligomerization triggers differential binding of a pore-forming toxin to a different receptor leading to efficient interaction with membrane microdomains. Biochim Biophys Acta. 2004; 1667:38–46. [PubMed: 15533304]
5. Gómez I, Dean DH, Bravo A, Soberón M. Molecular basis for *Bacillus thuringiensis* Cry1Ab toxin specificity: Two structural determinants in the *Manduca sexta* Bt-R_1 receptor interact with loops α-8 and 2 in domain II of Cy1Ab toxin. Biochemistry. 2003; 42:10482– 10489. [PubMed: 12950175]
6. Gómez I, Arenas I, Benitez I, Miranda-Ríos J, Becerril B, Grande R, Almagro JC, Bravo A, Soberón M. Specific epitopes of domains II and III of *Bacillus thuringiensis* Cry1Ab toxin involved in the sequential interaction with cadherin and aminopeptidase-N receptors in *Manduca sexta*. J Biol Chem. 2006; 281:34032–34039. [PubMed: 16968705]
7. Xie R, Zhuang M, Ross LS, Gómez I, Oltean DI, Bravo A, Soberón M, Gill SS. Single amino acid mutations in the cadherin receptor from *Heliothis virescens* affect its toxin binding ability to Cry1A toxins. J Biol Chem. 2005; 280:8416–8425. [PubMed: 15572369]
8. Gómez I, Sánchez J, Miranda R, Bravo A, Soberón M. Cadherin-like receptor binding facilitates proteolytic cleavage of helix α-1 in domain I and oligomer pre-pore formation of *Bacillus thuringiensis* Cry1Ab toxin. FEBS Lett. 2002; 513:242–246. [PubMed: 11904158]
9. Zhuang M, Oltean DI, Gómez I, Pullikuth AK, Soberón M, Bravo A, Gill SS. *Heliothis virescens* and *Manduca sexta* lipid rafts are involved in Cry1A toxin binding to the midgut epithelium and subsequent pore formation. J Biol Chem. 2002; 277:13863–13872. [PubMed: 11836242]

10. Hua G, Zhang R, Abdullah MA, Adang MJ. *Anopheles gambiae* cadherin AgCad1 binds the Cry4Ba toxin of *Bacillus thuringiensis israelensis* and a fragment of AgCad1 synergizes toxicity. Biochemistry. 2008; 47:5101–5110. [PubMed: 18407662]
11. Abdullah MA, Valaitis AP, Dean DH. Identification of a *Bacillus thuringiensis* Cry11Ba toxin-binding aminopeptidase from the mosquito, *Anopheles quadrimaculatus*. BMC Biochem. 2006; 7:16. [PubMed: 16716213]
12. Zhang R, Hua G, Andacht TM, Adang MJ. A 106-kDa aminopeptidase is a putative receptor for *Bacillus thuringiensis* Cry11Ba toxin in the mosquito *Anopheles gambiae*. Biochemistry. 2008; 47:11263–11272. [PubMed: 18826260]
13. Fernández LE, Aimanova KG, Gill SS, Bravo A, Soberón MA. GPI-anchored alkaline phosphatase is a functional midgut receptor of Cry11Aa toxin in *Aedes aegypti* larvae. Biochem J. 2006; 394:77–84. [PubMed: 16255715]
14. Abdullah MA, Alzate O, Mohammad M, McNall RJ, Adang MJ, Dean DH. Introduction of Culex toxicity into *Bacillus thuringiensis* Cry4Ba by protein engineering. Appl Environm Microbiol. 2003; 69:5343–5353.
15. Fernández LE, Pérez C, Segovia L, Rodríguez MH, Gill SS, Bravo A, Soberón M. Cry11Aa toxin from *Bacillus thuringiensis* binds its receptor in *Aedes aegypti* mosquito larvae trough loop α-8 of domain II. FEBS Lett. 2005; 579:3508–3514. [PubMed: 15963509]
16. Tuntitippawan T, Boonserm P, Katzenmeier G, Angsuthanasombat C. Targeted mutagenesis of loop residues in the receptor-binding domain of the *Bacillus thuringiensis* Cry4Ba toxin affects larvicidal activity. FEMS Microbiol Lett. 2005; 242:325–332. [PubMed: 15621455]
17. Pérez C, Muñoz-Garay C, Portugal LC, Sánchez J, Gill SS, Soberón M, Bravo A. *Bacillus thuringiensis* subsp. *israelensis* Cyt1Aa enhances activity of Cry11Aa toxin by facilitating the formation of a pre-pore oligomeric structure. Cell Microbiol. 2007; 9:2931–2937. [PubMed: 17672866]
18. Chang C, Yu YM, Dai SM, Law SK, Gill SS. High-level cryIVD and cytA gene expression in *Bacillus thuringiensis* does not require the 20-kilodalton protein, and the coexpressed gene products are synergistic in their toxicity to mosquitoes. Appl Environ Microbiol. 1993; 59:815–821. [PubMed: 8481007]
19. Lereclus D, Arantes O, Chaufaux J, Lecadet MM. Transformation and expression of a cloned δ-endotoxin gene in *Bacillus thuringiensis*. FEMS Microbiol Lett. 1989; 60:211–218. [PubMed: 2550317]
20. Lereclus D, Agaisse H, Gominet M, Chaufaux J. Overproduction encapsulated insecticidal crystal proteins in a *Bacillus thuringiensis* spoOA mutant. Bio/Technol. 1995; 13:67–71.
21. Thomas WE, Ellar DJ. *Bacillus thuringiensis* var *israelensis* crystal delta-endotoxin: effects on insect and mammalian cells *in vitro* and *in vivo*. J Cell Sci. 1983; 60:181–197. [PubMed: 6874728]
22. Herrera-Ortiz A, Lanz-Mendoza H, Martínez-Barnetche J, Hernández-Martínez S, Villarreal-Treviño, Aguilar-Marcelino L, Rodríguez MH. *Plasmodium berghei* ookinetes induce nitric oxide production in *Anopheles pseudopunctipennis* midguts cultured *in vitro*. Insect Biochem Mol Biol. 2004; 34:893–901. [PubMed: 15350609]
23. Jin X, Aimanova K, Ross LS, Gill SS. Identification, functional characterization and expression of a LAT type amino acid transporter from the mosquito *Aedes aegypti*. Insect Biochem Mol Biol. 2003; 33:815–827. [PubMed: 12878228]
24. Nielsen-LeRoux C, Charles JF. Binding of *Bacillus sphaericus* binary toxin to a specific receptor on midgut brush-border membranes from mosquito larvae. Eur J Biochem. 1992; 210:585–590. [PubMed: 1459140]
25. Kramer A, Schneider-Mergener J. Synthesis and screening of peptide libraries on continuous cellulose membrane supports. Methods Mol Biol. 1988; 87:25–39. [PubMed: 9523256]
26. Perera OP, Willis JD, Adang MJ, Jurat-Fuentes JL. Cloning and characterization of the Cry1Ac-binding alkaline phosphatase (HvALP) from *Heliothis virescens*. Insect Biochem Mol Biol. 2009; 39:294–302. [PubMed: 19552892]

27. De Backer M, McSweeney S, Rasmussen HB, Riise BW, Lindley P, Hough E. The 1.9Å crystal structure of heatlabile shrimp alkaline phosphatase. J Mol Biol. 2002; 318:1265–1274. [PubMed: 12083516]

28. Yamagiwa M, Ogawa R, Yasuda K, Natsuyama H, Sen K, Sakai H. Active form of dipteran-specific insecticidal protein cryllA produced by *Bacillus thuringiensis* subsp. *israelensis*. Biosci Biotechnol Biochem. 2002; 66:516–522. [PubMed: 12005043]

29. Jurat-Fuentes JL, Adang MJ. Characterization of a Cry1Ac-receptor alkaline phosphatase in susceptible and resistant *Heliothis virescens* larvae. Eur J Biochem. 2004; 271:3127–3135. [PubMed: 15265032]

30. Valaitis AP, Jenkins JL, Lee MK, Dean DH, Garner KJ. Isolation and partial characterization of Gypsy moth BTR-270 an anionic brush border membrane glycoconjugate that binds *Bacillus thuringiensis* Cry1A toxins with high affinity. Arch Insect Biochem Physiol. 2001; 46:186–200. [PubMed: 11304752]

31. Ochoa-Campuzano C, Real MD, Martínez-Ramírez AC, Bravo A, Rausell C. An ADAM metalloprotease is a Cry3Aa *Bacillus thuringiensis* toxin receptor. Biochem Biophys Res Commun. 2007; 362:437–442. [PubMed: 17714689]

32. Jenkins JL, Lee MK, Valaitis AP, Curtiss A, Dean DH. Bivalent sequential binding model of a *Bacillus thuringiensis* toxin to gypsy moth aminopeptidase N receptor. J Biol Chem. 2000; 275:14423–14431. [PubMed: 10799525]

33. Pardo-López L, Gómez I, Rausell C, Sánchez J, Soberón M, Bravo A. Structural changes of the Cry1Ac oligomeric pre-pore from *Bacillus thuringiensis* induced by *N*-acetylgalactosamine facilitates toxin membrane insertion. Biochemistry. 2006; 45:10329–10336. [PubMed: 16922508]

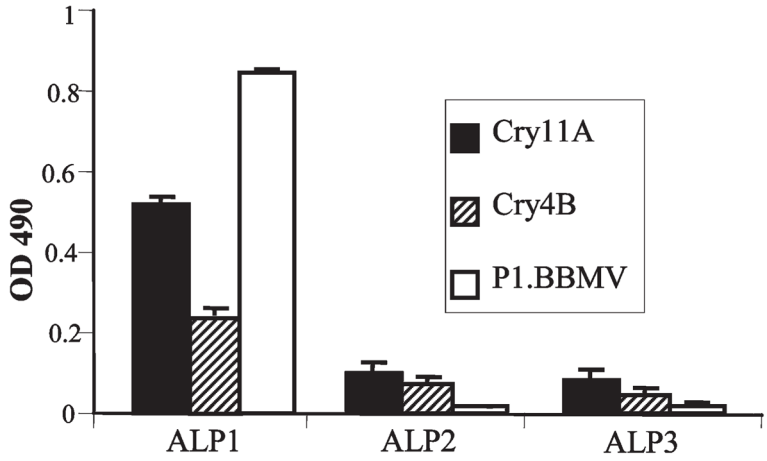

Figure 1.
ALP1 is involved in Cry11Aa binding. ELISA binding assays of recombinant alkaline phosphatase isoforms ALP1, ALP2, and ALP3 to Cry11Aa and Cry4Ba toxins and P1.BBMV peptide phage.

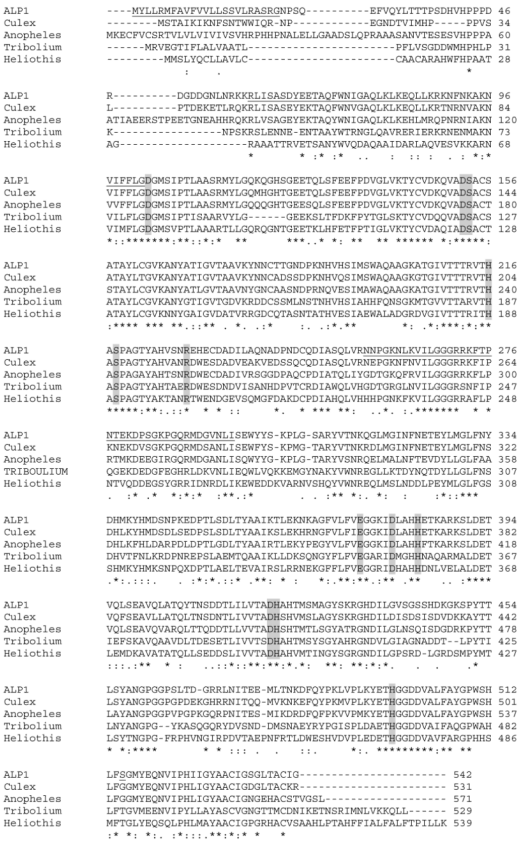

Figure 2.

Protein sequence alignment of membrane-bound midgut alkaline phosphatase from *Ae. aegyti* larvae (ALP1) with different insect ALP's. Conserved residues involved in catalysis or in metal binding are marked in gray. The amino-terminal signal peptide and the two Cry11Aa binding regions R59–G102 and N257–I296 are underlined. The nine overlapping peptide sequences correspond to the following ALP1 amino acid sequence: P1, S26–A176; P2, R59–T211; P3, D103–R256; P4, K148–Y301; P5, M196–E347; P6, P244–Q396; P7, S297–E446; P8, E347–T496; P9, L391–G542.

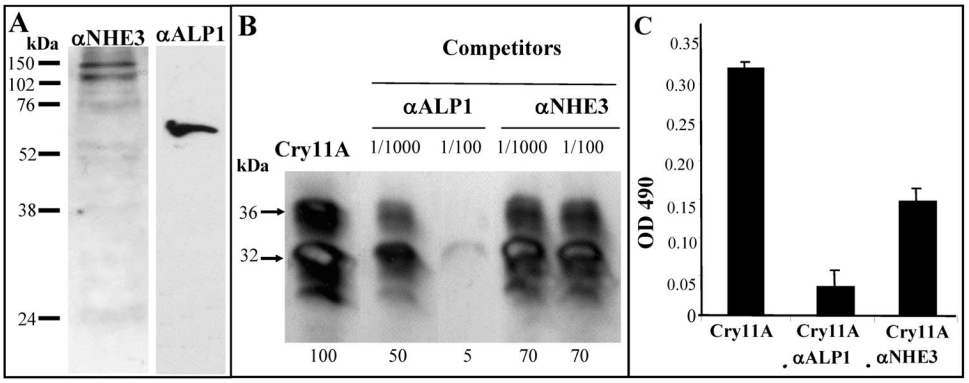

Figure 3.

ALP1 is involved in binding to BBMV and toxicity of Cry11Aa to *Ae. aegypti*. (A) Western blot of BBMV proteins detected with anti-ALP1 or anti-NHE3 antibodies. (B) Binding competition assay of 5 nM trypsin-activated Cry11Aa with 10 μg of BBMV in the presence of anti-ALP1 or anti-NHE3 antibodies at different dilutions of the antibodies (1:1000 or 1:100). Numbers in the bottom represent percentage of binding by scanning optical density of the 36 kDa band. (C) Lactate dehydrogenase release of isolated cultured *Ae. aegypti* guts in the presence ofCry11Aa protoxin with or without incubation with anti-ALP1 or anti-NHE3 antibodies. Three replicates of two guts per well for each treatment were analyzed.

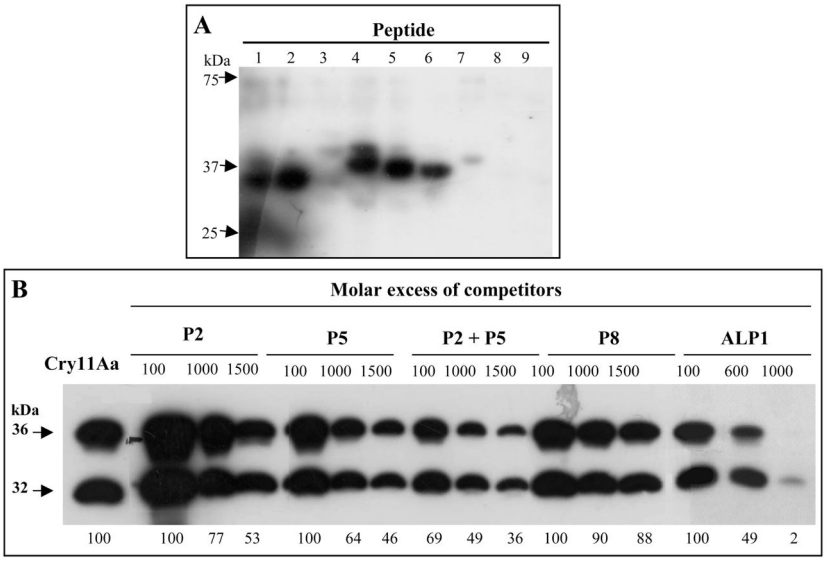

Figure 4.

Two binding sites in ALP1 are involved in Cry11Aa interaction. (A) Toxin overlay assays of blotted ALP1 overlapping peptides P1–P9 corresponding to lanes 1–9 revealed with Cry11Aa. (B) Binding competition assay of 5 nM trypsin-activated Cry11Aa with 10 μg of BBMV in the presence of different molar excess ofALP1 peptides P1, P5, P8, andALP1. Numbers in the bottom represent percentage of binding by scanning optical density of the 36 kDa band.

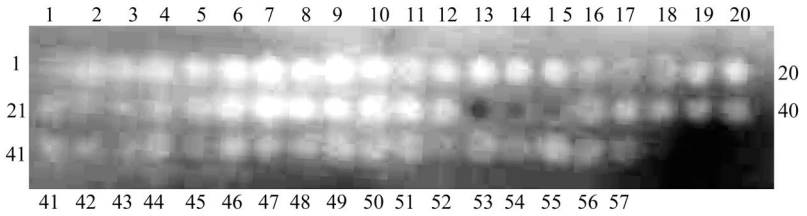

Figure 5.
Cry11Aa peptide-spot array of domain III amino acid sequence revealed with ALP1. Numbers in the figure were included to facilitate identification of the peptide spots in each row.

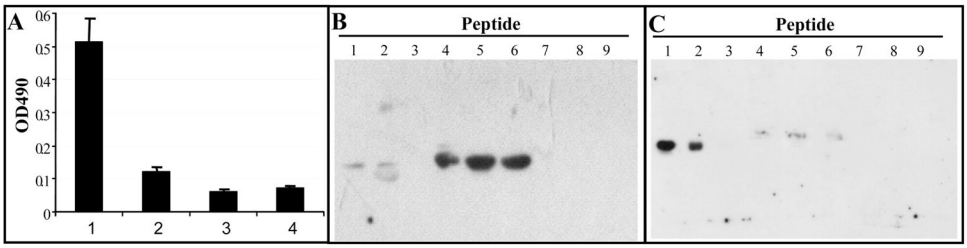

Figure 6.

Cry11Aa domain II loopα-8 and domain III β18-β19 regions are involved inALP1 binding. (A)ELISA binding assays of recombinant ALP1-TRX to different toxin proteins: Cry11Aa (lane 1), Cry11Aa E266A (lane 2), Cry11Aa QSQ563–565AAA (lane 3), and NSG566–568AAA (lane 4). (B) Toxin overlay assays of blotted ALP1 overlapping peptides P1–P9 corresponding to lanes 1–9 revealed with Cry11Aa E266A mutant toxin. (C) Toxin overlay assays of blotted ALP1 overlapping peptides P1–P9 corresponding to lanes 1–9 revealed with Cry11Aa QSQ563–565AAA mutant toxin.

Table 1

Oligonucleotides Used for Amplification and Cloning of the Nine ALP1 Overlapping Sequences

name of peptide and ALP1 amino acid sequence	oligonucleotide sequence
P1, S26–A176	ALPF1bgl-f: 5′-GAA GAT CTA TCG CAG GAA TTC GTC C-3′ ALPF1-r: 5′-ACC AAG CTT GGG TAT ATT TGA CCG CAG CCG TC-3′
P2, R59–T211	ALPF2bgl-f: 5′-GAA GAT CTG AGA CTG ATT TCC GCG TCG-3′ ALPF2-r: 5′-ACC AAG CTT GGG GGT GGT CAC AAT GCC TGT GGC-3′
P3, D103–R256	ALPF3bgl-f: 5′-GAA GAT CTA GAT GGC ATG CTG ATT CCG-3′ ALPF3-r: 5′-ACC AAG CTT GGG TCG CAC GAG TTG GGA TGC-3′
P4, K148–Y301	ALPF4bgl-f: 5′-GAA GAT CTT AAG CAG GTT GCA GAT TCG-3′ ALPF4-r: 5′-ACC AAG CTT GGG ATA GTA CCA TTC CGA GAT C-3′
P5, M196–E347	ALPF5bgl-f: 5′-GAA GAT CTC ATG AGC TGG GCT C-3′ ALPF5-r: 5′-ACC AAG CTT GGG CTT CTT TTG TGT TGC TGT CC-3′
P6, P244–Q396	ALPF6bgl-f: 5′-GAA GAT CTT CCA AAT GAC TGC CAA GAC-3′ ALPF6-r: 5′-ACC AAG CTT GGG ACC GTT TCG TCC AGG GAT TTC-3′
P7, S297–E446	ALPF7bgl-f: 5′-GAA GAT CTC TCG GAAT GGT ACT ATA GC-3′ ALPF7-r: 5′-ACC AAG CTT GGG TTG TCG TGG GAT GAA CC-3′
P8, E347–T496	ALPF8bgl-f: 5′-GAA GAT CTA GAA GAC CCC ACC CTA AGC-3′ ALPF8-r: 5′-ACC AAG CTT GGG GGT TTC GTA CTT CAA AGG-3′
P9, L391–G542	ALPF9bgl-f: 5′-GAA GAT CTC CTG GAC GAA ACG GTC-3′ ALPF9-r: 5′-ACC AAG CTT GGG CCC TAT GCA CGC CGT TAA TCC-3′

Table 2

Biological Activity of Cry11Aa Mutant Proteins to *Ae. aegypti* Larvae[a]

toxin	LC_{50}[b] (ng/mL)
Cry11Aa	324.12 (245–376)[b]
Cry11Aa QSQ563–565AAA	881.7 (803–1250)
Cry11Aa NSG566–568AAA	1019.5 (910–1720)

[a]Bioassays were performed with 10 early fourth-instar *Ae. aegypti* larvae in 100 mL of H_2O per dose. Three independent experiments of ten different doses each were done. Mean lethal concentration (LC_{50}) was estimated by Probit analysis.

[b]95% confidence limits are given in parentheses.